SECED 2023 Conference
Earthquake Engineering & Dynamics for a Sustainable Future
14-15 September 2023, Cambridge, UK

SEISMIC HAZARD ASSESSMENT OF THE SAN RAMÓN FAULT IN SANTIAGO, CHILE

Horacio DOMÍNGUEZ[1] & Pablo HERESI[2]

Abstract: *The seismic hazard in Chile is primarily controlled by interface and inslab earthquakes that occur due to the subduction of the Nazca Plate beneath the South American Plate. However, recent discoveries of seismic activity on the San Ramón Fault (SRF), an active shallow crust thrust fault system located at the eastern border of the city of Santiago, present a new seismic hazard scenario for the city. The SRF has a slip rate of approximately* $0.4\ [mm/year]$ *and is capable of generating earthquakes with magnitudes up to* $M_w 7.5$*. Although the seismic hazard posed by the SRF has been studied previously, a probabilistic analysis has not been performed yet. In this context, this research compares the seismic hazard generated by the subduction zone (i.e., interface and inslab events) with the hazard generated by the SRF in Santiago, using models that represent the geometry and potential seismicity of each source. We compute seismic hazard maps of Santiago using deterministic and probabilistic approaches to assess the influence of the SRF. Resulting maps from a deterministic approach present regions where the intensities produced by an earthquake on the SRF can duplicate the ones generated by interface and inslab events. However, due to the low recurrence period of the fault, a probabilistic approach indicates that the effect of the SRF on the seismic hazard in Santiago is less than 5% of the hazard generated by the subduction zone. These results provide evidence for future modifications of seismic codes in Chile.*

Introduction

Chile is well-known due to its very high seismicity, which includes megathrust events such as the 1960 Valdivia Earthquake, $M_w 9.6$ (Cifuentes and Silver, 1989) and the 2010 Maule Earthquake, $M_w 8.8$ (Vigny et al., 2011). The country's seismic activity is primarily due the subduction zone of the Nazca Plate beneath the South American Plate. Santiago, the capital city of Chile, is home to approximately seven million people and represents the economic center of the country. Despite its economic significance, Santiago has been struck by several earthquakes throughout its history. These events include the 1906 Valparaíso Earthquake, $M_w 8.2$ (Astroza, 2007), the 1939 Chillán Earthquake, $M_w 7.8$ (Campos and Kausel, 1990), the 1965 La Ligua Earthquake, $M_w 7.4$ (Norambuena, 2006), the 1985 Algarrobo Earthquake, $M_w 8.0$ (Comte et al., 1986), and the 2010 Maule Earthquake, $M_w 8.8$ (Vigny et al., 2011), all of them causing structural damage and significant losses to the city.

The San Ramón Fault is an active shallow crust thrust fault system located at the piedmont of Los Andes Mountain range, on the eastern border of Santiago. The fault trace is $30\ [km]$ long, 55% of which has been urbanized (Easton et al. 2018), yet it is possible that the trace extends $20\ [km]$ further to the south (Ammirati et al., 2019). Using paleoseismology techniques, Vargas et al. (2014) identified that two events of magnitude $\sim M_w 7.5$ occurred in the past $17{,}000 - 19{,}000$ years. Shallow earthquakes, similar to those that could be nucleated in the San Ramón Fault, have caused major losses worldwide. For example, the 1995 Kobe, Japan Earthquake, $M_w 7.2$ (Kanaori and Kawakami, 1996), the 1999 Chi-Chi, Taiwan Earthquake, $M_w 7.6$ (Shin and Teng, 2001), and the recent event of Kahramanmaras, Turkey, $M_w 7.8$, (Dilsiz et al., 2023) caused the collapse of several structures in the nearby regions. Given the San Ramón Fault's location and its potential seismic activity, accurately characterizing its seismic hazard is crucial for the safety of Santiago.

Although the seismic hazard of the San Ramón Fault has been studied previously within a deterministic approach (Estay et al., 2016; Ammirati et al., 2019), it has not been analyzed using a probabilistic approach. Moreover, the seismic hazard of the fault has not been compared to the

[1] Graduate Student, Universidad Técnica Federico Santa María, Santiago, Chile, horacio.dominguez@sansano.usm.cl
[2] Assistant Professor, Universidad Técnica Federico Santa María, Santiago, Chile.

hazard generated by subduction events (i.e., both interface and inslab). Given that seismic design codes of Chile use hazard maps that only consider interface events, this comparison is relevant to understand the potential underestimation of the seismic hazard in Santiago.

In this article, we aim to compare the seismic hazard generated by subduction events (i.e., interface and inslab) with the hazard posed by the San Ramón Fault. We estimate response spectra and seismic hazard maps using state-of-the-art geometries and seismic potential. This analysis enables us to identify the regions of Santiago where the influence of the San Ramón Fault is greater than that of subduction events. These zones will be referred as influence zones hereafter.

The San Ramón Fault

The San Ramón Fault was first studied by Brüggen (1950). However, it was not until 2002 that it was identified as an active fault (Rauld, 2002). This was later confirmed by various authors (Estay et al. 2016; Pérez et al. 2014; Vargas et al. 2014). In this context, several studies have been conducted using various techniques, such as paleoseismology (Vargas et al., 2014), analysis of geomorphological and geophysical evidence (Armijo et al., 2010) and detection of hypocenters of minor events (Pérez et al., 2014; Estay et al., 2016; Ammirati et al., 2019) to describe its seismic and geometrical characteristics.

The geometry of the San Ramón Fault still has a great uncertainty. Its trace is believed to be $30\ [km]$ long (Pérez et al., 2014), yet it could be composed of four independent $10\ [km]$ long segments (Estay et al., 2016) or even have $50\ [km]$ of total extension (Ammirati et al., 2019). Its width could range between $10\ [km]$ (Estay et al., 2016) and $40\ [km]$ (Armijo et al., 2010) and its dip between $30°$ (Pérez et al., 2014) and $65°$ (Estay et al., 2016). A similar issue occurs with its potential seismicity; the recurrence of the fault was proposed to be approximately between $2{,}500$ and $10{,}000$ years by Armijo et al. (2010), based on the slip rate of the fault. However, two events detected approximately $8{,}000$ and $17{,}000 - 19{,}000$ years ago by Vargas et al. (2014) suggest a recurrence period of $9{,}000 \pm 500$ years. Finally, the maximum magnitude of an event within the San Ramón Fault has been computed in accordance with the fault's length and width proposed by each author, ranging between $M_w 6.2$ and $M_w 7.5$.

Despite of the seismic hazard that the San Ramón Fault can pose to Santiago, over 55% of its trace has been urbanized (Easton et al., 2018), and there are three hospitals and a nuclear study center within a distance of $2\ [km]$ from the fault. The study of the San Ramón Fault is even more important when considering that is one of the largest active shallow crust faults of Chile and one of the farthest from the subduction trench. This means that its influence zone is expected to be an upper bound for other similar faults in Chile.

Methodology

To compute seismic hazard maps, the study zone considered is the one investigated by Acevedo (2021). The author estimated the time-averaged shear wave velocity in the top $30\ [m]$ of soil, V_{S30}, and the fundamental period of 44 sites between coordinates $70.50° - 70.96°W$ and $33.33° - 33.72°S$ (Figure 1). The seismic hazard is determined on every site to obtain hazard maps using both a deterministic seismic hazard analysis (*DSHA*) and a probabilistic seismic hazard analysis (*PSHA*). Also, a map presenting the ratio of the hazard of the San Ramón Fault and subduction events is determined. In this map, ratio values greater than 1 represent the influence zone of the fault (i.e., the hazard posed by the fault is greater than the hazard generated by subduction events). Two test sites are selected to estimate pseudo-acceleration response spectra from a *DSHA* and uniform hazard spectra from a *PSHA*. Site 1 is in the municipality of Ñuñoa, $33.47°S$ $70.61°W$, $8.5\ [km]$ to the west of the fault trace, whereas Site 2 is located over the San Ramón Fault trace, $33.47°S$ $70.52°W$ (Figure 2). Site 1 has a period of $0.77\ [s]$ and a V_{s30} of $579\ [m/s]$, while Site 2 has a period of $0.39\ [s]$ and a V_{s30} of $415\ [m/s]$.

Ground motion models are selected using the criteria proposed by Bommer et al. (2010). For active shallow crust events, both ASB14 (Akkar, Sandıkkaya and Bommer, 2014) and BSSA14 (Boore et al., 2014) are combined in a logic tree with equal weights. For interface events, the models AG20 (Abrahamson and Gulerce, 2022), IRRP17 (Idini et al., 2017) and MBR17 (Montalva, Bastías and Rodriguez-Marek, 2017) are combined in a logic tree with equal weights. Finally, for inslab events we only consider AG20 (Abrahamson and Gulerce, 2022) and MBR17

(Montalva, Bastías and Rodriguez-Marek, 2017) with equal weights. The IRRP17 model was not considered for inslab events due to its poor constraint for large-magnitude inslab earthquakes.

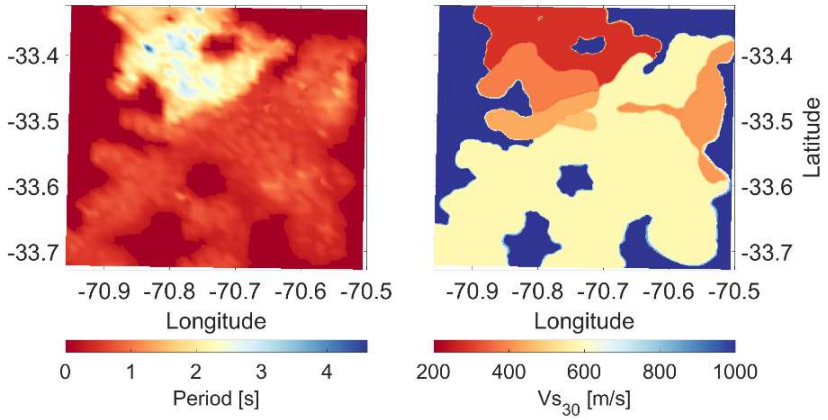

Figure 1. Site parameters of the study zone (Acevedo, 2021).

Specifics for a Deterministic Seismic Hazard Analysis

Based on a worst-case scenario criteria, a $M_w 7.5$ event is considered on the San Ramón Fault, in relation to a rupture of $50\ [km]$, according to the fault trace length proposed by Ammirati et al. (2019), and a width of $20\ [km]$. For the interface event, a $M_w 9.3$ event is considered, as it is the maximum magnitude of the zone according to Poulos et al. (2019). The rupture of this event is located in front of Santiago, using the *Slab2* model (Hayes et al., 2018). Finally, a $M_w 7.8$ event is considered for the inslab scenario, with its hypocenter located at a depth of $71\ [km]$ under Santiago, based on the *Slab2* model (Hayes et al., 2018) at coordinates $33.51°S\ 70.67°W$. Figure 2 presents the trace of the San Ramón Fault, the considered rupture of the interface event, the epicenter of the inslab event, and the two specific sites of study.

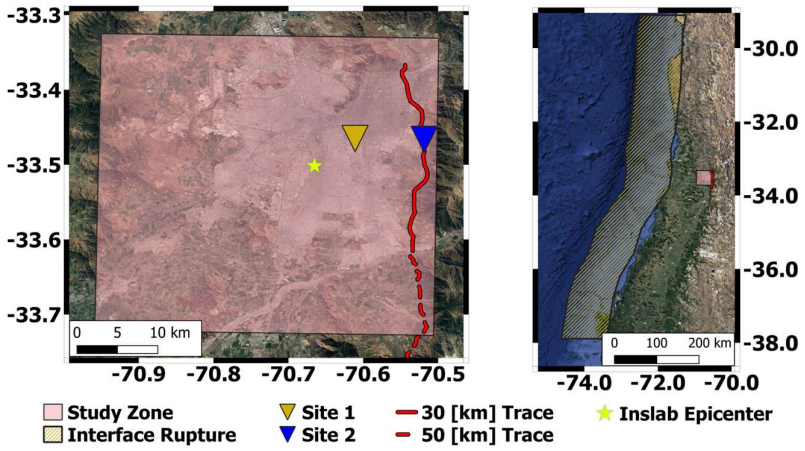

Figure 2. Map of the study zone to compute seismic hazard maps and the two test sites to compute response spectra. Red lines indicate the trace of the San Ramón Fault, the star represents the epicenter of the inslab event and the yellow dashed zone represents the interface rupture.

Specifics for a Probabilistic Seismic Hazard Analysis

The geometric model of the San Ramón Fault considered for a *PSHA* is the same as the one considered in the *DSHA*. However, its extension is divided into two possible values, 30 and $50\ [km]$ combined with weights of 0.6 and 0.4 in a logic tree analysis. Due to differences on the average slip of the fault, the maximum magnitude of the $30\ [km]$ fault trace branch is also split into two values, $M_w 7.1$ and $M_w 7.3$ both with a weight of 0.5. The $50\ [km]$ fault trace branch is

associated only to a maximum magnitude of $M_w 7.5$. The fault is considered to have a Characteristic Event recurrence model (Schwartz and Coppersmith, 1984), where all previous branches are separated into three new sub-models according to the recurrence period assigned: $8{,}500$, $9{,}000$ and $9{,}500$ years, with corresponding weights of 0.25, 0.50 and 0.25, respectively. The lowest maximum magnitude considered in all nine resulting branches is $M_w 6.7$, which is the value proposed by Estay et al. (2016).

The subduction zone is modeled using the results of two previous studies. The geometry is obtained from the *Slab2* model (Hayes et al., 2018). Moreover, the potential seismicity of the subduction zone is considered using the recurrence models proposed by Poulos et al. (2019), who divided the subduction zone into three interface zones and four inslab zones and computed bounded Guthemberg-Richter recurrence models for each one.

Results

Results from a Deterministic Seismic Hazard Analysis

The *DSHA* is computed considering magnitudes $M_w 7.5$ for the San Ramón Fault, $M_w 9.3$ for the interface event and $M_w 7.8$ for the inslab event. Figure 3 presents the response spectra obtained at both test sites, where a greater intensity is generated by the inslab event for short periods at both sites. As can be seen in Figure 3, at Site 1 the San Ramón Fault produces higher intensities than both subduction events for vibration periods over $0.8\ [s]$. Hence, the influence zone of the San Ramón Fault must reach this site for vibration periods over $0.8\ [s]$. For Site 2, the San Ramón Fault generates much higher intensities than both subduction events for vibration periods over $0.25\ [s]$.

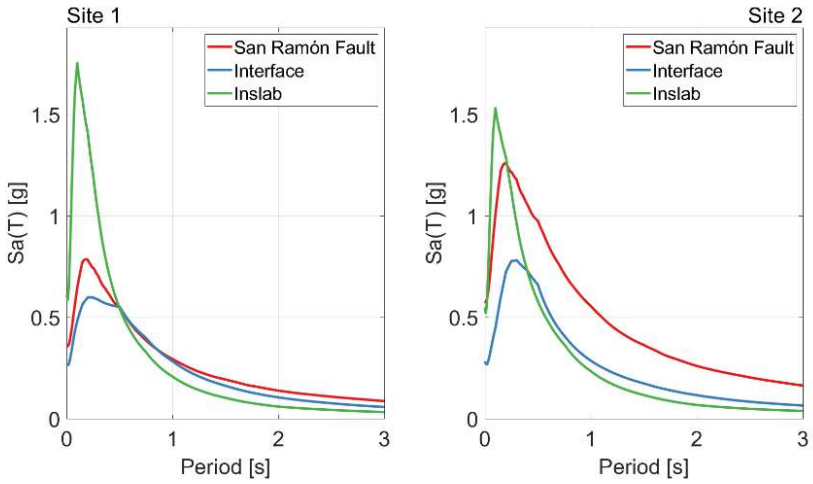

Figure 3. Pseudo-acceleration response spectra obtained from a Deterministic Seismic Hazard Analysis, considering magnitudes of $M_w 7.5$ for the San Ramón Fault, $M_w 9.3$ from the interface event and $M_w 7.8$ from the inslab event (see Figure 2 for locations of ruptures and test sites).

Figure 4 shows seismic hazard maps generated from the *DSHA*. In particular, it shows the median intensity for spectral pseudo-acceleration ordinates at a vibration period of $1\ [s]$, $Sa(1\ [s])$, for: (a) the San Ramón Fault; and (b) the envelope of both subduction events. The bottom panel of Figure 4 shows the ratio between the intensity produced by the San Ramón Fault and subduction events.

As can be seen in Figure 4 (top panel), the San Ramón Fault hazard map indicates that a $M_w 7.5$ event could cause spectral pseudo-accelerations greater than $0.5\ [g]$ on the nearby sites, yet it decreases rapidly with increasing source-to-site distance (i.e., to the west of the fault). On the other hand, the subduction envelope hazard map (middle panel of Figure 4) shows more stable values of intensities, which range between $0.3 - 0.4\ [g]$, controlled mainly by site characteristics (i.e., V_{S30} and fundamental period of the site).

The hazard ratio map (bottom panel of Figure 4) displays an influence zone of the San Ramón Fault reaching up to $9\ [km]$ to the west of its trace, hardly covering Site 1. Note that at sites

located closer than $1\ [km]$ from the San Ramón Fault, intensities due to an earthquake on the fault can duplicate the ones generated by the subduction events.

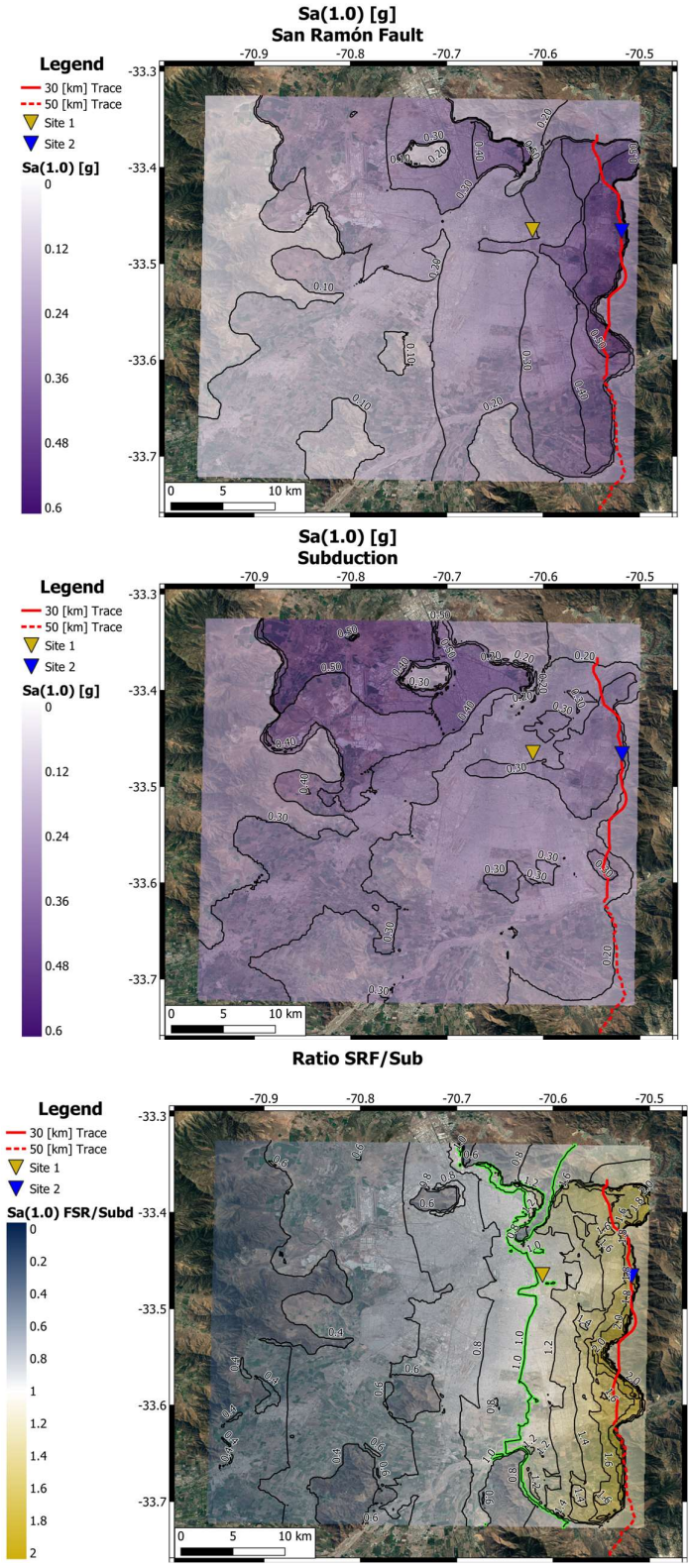

Figure 4. Seismic hazard maps for $Sa(1\ [s])$ computed from a DSHA. Top: $M_w 7.5$ event on the San Ramón Fault. Middle: Envelope of $M_w 9.3$ interface and $M_w 7.8$ inslab events. Bottom: Ratio between San Ramón Fault and subduction intensities. See Figure 2 for locations of ruptures.

Results from a Probabilistic Seismic Hazard Analysis

Uniform hazard spectra were computed considering probabilities of exceedance of 10%, 2%, 0.5% and 0.25% in 50 years. These values are associated with return periods of 475, $2{,}475$, $9{,}975$ and $19{,}975$ years, respectively. Figure 5 shows the uniform hazard spectra at both test sites considering (a) the hazard posed by the San Ramón Fault and subduction events; and (b) only the interface and inslab hazard.

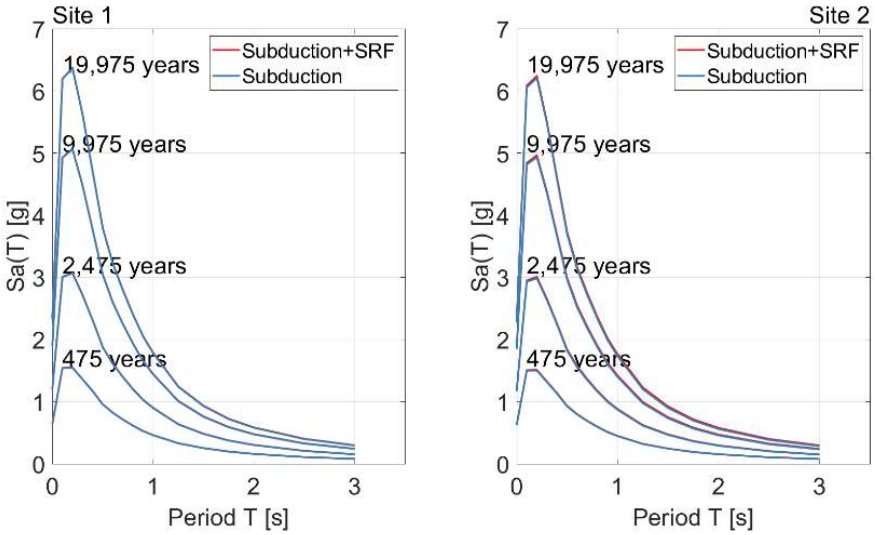

Figure 5. Uniform hazard spectra obtained from a Probabilistic Seismic Hazard Analysis at both test sites (see Figure 2 for their locations) for subduction + San Ramón Fault (SRF) hazard and for only subduction hazard.

Compared to the results from a *DSHA*, the uniform hazard spectra presented in Figure 5 suggest a completely different scenario regarding the influence of the San Ramón Fault. Both curves, considering and neglecting the fault, are almost identical, even at Site 2, which is located just on top of the fault. Thus, from a probabilistic approach, the seismic hazard generated by the San Ramón Fault is almost negligible in comparison with the one posed by subduction events. The influence of the fault slightly increases (yet it remains negligible) as the return period increases, specially at Site 2 and for very long return periods (>$10{,}000$ years), due to its long recurrence period of $9{,}000 \pm 500$ years.

Figure 6 shows seismic hazard maps from a *PSHA*. These maps show the probability of exceeding a spectral value $Sa(1\ [s])$ of $1\ [g]$ in 50 years, considering: (a) only the San Ramón Fault; and (b) only interface and inslab events. The bottom panel of Figure 6 presents the ratio between the probabilities obtained in the previous maps. These maps confirm the negligible levels of hazard generated by the San Ramón Fault when compared to the subduction events. The maximum probability of exceedance in 50 years reached by the San Ramón Fault within the study zone (top panel of Figure 6) is less than 0.07%, meaning a return period over $71{,}000$ years. In particular, at Site 1 the probability of exceedance in 50 years is less than 0.04%, equivalent to a return period greater than $166{,}000$ years. On the other hand, the subduction events map (middle panel of Figure 6) show a maximum of 2% on the northwestern region of the study zone. At the proximities of the San Ramón Fault trace, the probability of exceedance in 50 years decreases to a 1.4%, equivalent to a return period of $3{,}500$ years, 20 times smaller than the one computed considering only the seismic hazard posed by the San Ramón Fault.

Contrary to the *DSHA*, the hazard ratio map from a *PSHA* (bottom panel of Figure 6) shows an absence of influence zone of the San Ramón Fault. In particular, the probability of exceedance in 50 years generated by the fault reaches a maximum of a 5% of the one due to subduction events. This ratio is consistent with the ratio of return periods previously mentioned.

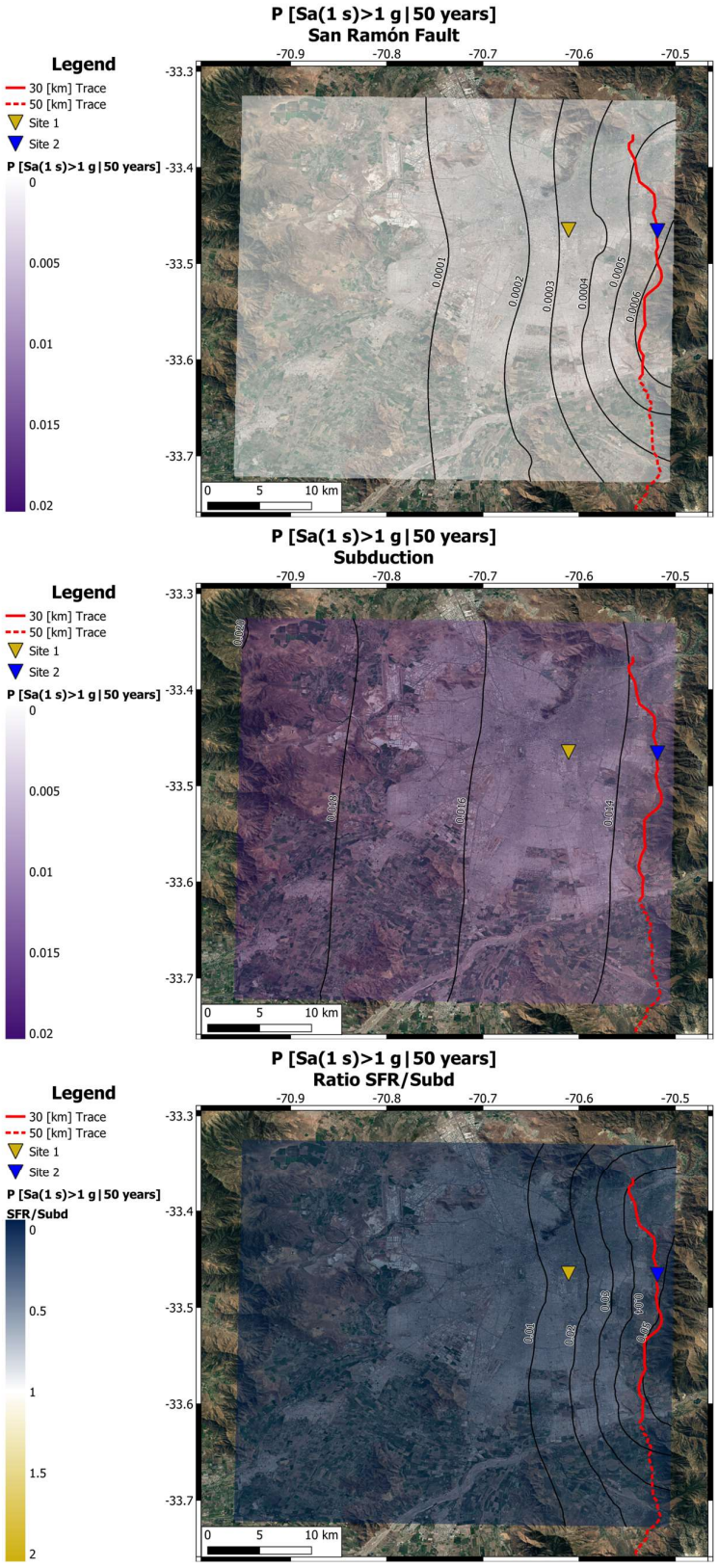

Figure 6. Seismic hazard maps obtained from a PSHA, displaying the probability that $Sa(1\ [s])$ exceeds $1\ [g]$ in 50 years for the San Ramón Fault (Top) and subduction events (Middle). Bottom: Ratio between the probabilities obtained for the San Ramón Fault and subduction events.

Conclusions

The assessment of the seismic hazard posed by the San Ramón Fault is crucial to Santiago, the capital city of Chile, due to its high urbanization and the importance of some structures near to its trace. The San Ramón Fault is capable of reaching magnitudes of $M_w 7.5$ and is one of the furthest shallow faults from the subduction trench in Chile, making its influence zone an upper bound for other similar faults in the country. In this context, this article presents a comparison of the seismic hazard in Santiago posed by the San Ramón Fault against that generated by interface and inslab events, using both a deterministic and probabilistic approaches.

Results from a Deterministic Seismic Hazard Analysis (*DSHA*) show that the influence zones of the San Ramón Fault (i.e., region within the city where the San Ramón Fault produces a higher hazard than that of interface/inslab events) depend on the considered ground-shaking intensity measure (i.e., vibration period of spectral acceleration). In this case, influence zones exist only for spectral accelerations with vibration periods greater than $0.3\ [s]$. In particular, for a vibration period of $1.0\ [s]$, the influence zone reaches $9\ [km]$ to the west of the fault trace. In this analysis, the intensity ratio between events on the San Ramón Fault and interface/inslab earthquakes is over 2.0 at sites near the fault.

In a *DSHA*, the probability of occurrence of different earthquakes is not explicitly considered. When these uncertainties are explicitly accounted for within a Probabilistic Seismic Hazard Analysis (*PSHA*), no influence zones of the San Ramón Fault are observed. In particular, the probability of the spectral acceleration for a vibration period of $1\ [s]$ exceeding a value of $1\ [g]$, is about 20 times larger when considering only the hazard posed by the subduction events, compared to the one posed by the San Ramón Fault. In other words, within a probabilistic approach, the seismic hazard posed by the San Ramón Fault is significantly lower than that of interface/inslab events.

The same methodology used in this work for a vibration period of $1\ [s]$ was used to evaluate the seismic hazard considering different vibration periods and intensity levels. Results from both *DSHA* and *PSHA* are similar to the results obtained in this article. Although these results are not shown herein due to space limitations, similar conclusions can be drawn from them.

Geometrical and seismic characteristics of the San Ramón Fault have great epistemic uncertainties and are still under study. Therefore, results of this investigation should be interpreted with caution. The *DSHA* results assume an extension of $50\ [km]$ of the fault trace, although it has been proposed to have $30\ [km]$ or even be divided into four segments of $10\ [km]$. Also, the dip angle and the rupture width are chosen as the median values of the range proposed by different authors. Similarly, the *PSHA* uses a Characteristic Event recurrence model for the San Ramón Fault, which greatly affects the seismic hazard. Therefore, the seismic activity of the San Ramón Fault should be carefully studied to improve our estimation of a recurrence law and thus, a more accurate hazard assessment. Considering that the recurrence period of the San Ramón Fault is approximately $9{,}000$ years and the last event occurred $8{,}000$ years ago, a non-Poissonian recurrence model would be probably better suited for the analysis. The authors of this article are currently working on these analyses.

References

Abrahamson NA and Gulerce Z (2022), Summary of the Abrahamson and Gulerce NGA-SUB ground-motion model for subduction earthquakes, *Earthquake Spectra*, 38(4): 2638–2681. doi: 10.1177/87552930221114374.

Acevedo M (2021), *Modelo de velocidades de la Cuenca de Santiago y estimación de su respuesta sísmica*, M.Sc. Thesis, Universidad de Chile, Chile

Akkar S, Sandıkkaya MA and Bommer JJ (2014), Empirical ground-motion models for point- and extended-source crustal earthquake scenarios in Europe and the Middle East, *Bulletin of Earthquake Engineering*, 12(1): 359–387. doi: 10.1007/s10518-013-9461-4.

Ammirati JB, Vargas G, Rebolledo S, Abrahami R, Potin B, Leyton F and Ruiz S (2019), The crustal seismicity of the western Andean thrust (Central Chile, 33°-34° s): Implications for regional tectonics and seismic hazard in the Santiago area, *Bulletin of the Seismological Society of America*, 109(5): 1985–1999. doi: 10.1785/0120190082.

Armijo R, Rauld R, Thiele R, Vargas G, Campos J, Lacassin R and Kausel E (2010), The West

Andean Thrust, the San Ramón Fault, and the seismic hazard for Santiago, Chile, *Tectonics*, 29(2): TC2007 doi: 10.1029/2008tc002427.

Astroza M (2007), Reinterpretación de las intensidades del terremoto de 1906, *VI Congreso Chileno de Geotecnia,* Valparaíso, Chile.

Bommer JJ*,* Douglas J, Scherbaum F, Cotton F, Bungum H and Fäh D (2010), On the selection of ground-motion prediction equations for seismic hazard analysis, *Seismological Research Letters*, 81(5): 783–793. doi: 10.1785/gssrl.81.5.783.

Boore DM, Stewart JP, Seyhan E, and Atkinson GM (2014), NGA-West2 equations for predicting PGA, PGV, and 5% damped PSA for shallow crustal earthquakes, *Earthquake Spectra*, 30(3): 1057–1085. doi: 10.1193/070113EQS184M.

Brüggen J (1950), *Fundamentos de la Geología en Chile,* 1st Ed., Santiago: Instituto Geográfico Militar.

Campos J and Kausel E (1990), The large 1939 intraplate earthquake of southern Chile, Seismological, *Seismological Research Letters,* 63: 43.

Cifuentes IL and Silver PG (1989), Low-frequency source characteristics of the great 1960 Chilean earthquake, *Journal of Geophysical Research*, 94(B1): 643–663. doi: 10.1029/JB094iB01p00643.

Comte D, Eisenberg A, Lorca E, Pardo M, Ponce L, Saragoni R, Singh SK and Suárez G (1986), The 1985 Central Chile earthquake: A repeat of previous great earthquakes in the region?, *Science*, 233(4762): 449–453. doi: 10.1126/science.233.4762.449.

Dilsiz A, Gunay S, Mosalam K, Miranda E, Arteta C, Sezen H, Fischer E, Hakhamaneshi M, Hassan W, ALhawamdeh B, Andrus S, Archbold J, Arslanturkoglu S, Bektas N, Ceferino L, Cohen J, Duran B, Erazo K, Faraone G, Feinstein T, Gautam R, Gupta A, Haj Ismail S, Jana A, Javadinasab Hormozabad S, Kasalanati A, Kenawy M, Khalil Z, Liou I, Marinkovic M, Martin A, Merino Y, Mivehchi M, Moya L, Pájaro Miranda C, Quintero N, Rivera J, Romão X, Lopez Ruiz MC, Sorosh S, Vargas L, Velani PD, Wibowo H, Xu S, Yilmaz T, Alam M, Holtzer G, Kijewski-Correa T, Robertson I, Roueche D and Safiey A (2023), *StEER: 2023 Mw 7.8 Kahramanmaras, Türkiye Earthquake Sequence Preliminary Virtual Reconnaissance Report (PVRR)*, StEER Structural Extreme Events Reconnaissance. DesignSafe-CI doi: https://doi.org/10.17603/ds2-7ry2-gv66.

Easton G, Inzulza J, Pérez S, Ejsmentewicz D and Jiménez C (2018), ¿Urbanización fallada? La Falla San Ramón como nuevo escenario de riesgo sísmico y la sostenibilidad de Santiago, Chile, *Revista de Urbanismo*, 38: 1–20.

Estay NP, Yáñez G, Carretier S, Lira E and Maringue J (2016), Seismic hazard in low slip rate crustal faults, estimating the characteristic event and the most hazardous zone: Study case San Ramón Fault, in southern Andes, *Natural Hazards and Earth System Sciences*, 16(12): 2511–2528. doi: 10.5194/nhess-16-2511-2016.

Hayes GP, Moore GL, Portner DE, Hearne M, Flamme H, Furtney M and Smoczyk GM (2018), Slab2 , a comprehensive subduction zone geometry model, *Science*, 362(6410): 58–61.

Idini B, Rojas F, Ruiz S and Pastén C (2017), Ground motion prediction equations for the Chilean subduction zone, *Bulletin of Earthquake Engineering*, 15(5): 1853–1880. doi: 10.1007/s10518-016-0050-1.

Kanaori Y and Kawakami SI (1996), The 1995 7.2 magnitude Kobe earthquake and the Arima-Takatsuki tectonic line: implications of the seismic risk for central Japan, *Engineering Geology*, 81(C): 61–82. doi: 10.1016/S0165-1250(97)80006-5.

Montalva GA, Bastías N and Rodriguez-Marek A (2017), Ground-motion prediction equation for the Chilean subduction zone, *Bulletin of the Seismological Society of America*, 107(2): 901–911. doi: 10.1785/0120160221.

Norambuena A (2006), *Estudio de los efectos del terremoto de La Ligua del 28 de marzo de 1965,* B.S.E Thesis, Universidad de Chile, Chile.

Pérez A, Ruiz JA, Vargas G, Rauld R, Rebolledo S and Campos J (2014), Improving seismotectonics and seismic hazard assessment along the San Ramón Fault at the eastern

border of Santiago city, Chile, *Natural Hazards*, 71(1): 243–274. doi: 10.1007/s11069-013-0908-3.

Poulos A, Monsalve M, Zamora N, de la Llera JC (2019), An updated recurrence model for chilean subduction seismicity and statistical validation of its poisson nature, *Bulletin of the Seismological Society of America*, 109(1): 66–74. doi: 10.1785/0120170160.

Rauld R (2002), *Análisis morfoestructural del frente cordillerano de Santiago Oriente, entre el río Mapocho y la quebrada de Macul*, B.S.E Thesis, Universidad de Chile, Chile.

Schwartz DP and Coppersmith KJ (1984), Fault behavior and characteristic earthquakes: Examples from the Wasatch and San Andreas Fault Zones, *Journal of Geophysical Research: Solid Earth*, 89(B7): 5681–5698. doi: https://doi.org/10.1029/JB089iB07p05681.

Shin TC and Teng TL (2001), An overview of the 1999 Chi-Chi, Taiwan, earthquake, *Bulletin of the Seismological Society of America*, 91(5): 895–913. doi: 10.1785/0120000738.

Vargas G, Klinger Y, Rockwell TK, Forman SL, Rebolledo S, Baize S, Lacassin R and Armijo R (2014), Probing large intraplate earthquakes at the west flank of the Andes, *Geology,* 42(12): 1083–1086. doi: 10.1130/G35741.1.

Vigny C, Socquet A, Peyrat S, Ruegg JC, Métois M, Madariaga R, Morvan S, Lancieri M, Lacassin R, Campos J, Carrizo D, Bejar-Pizarro M, Barrientos S, Armijo R, Aranda C, Valderas-Bermejo MC, Ortega I, Bondoux F, Baize S, Lyon-Caen H, Pavez A, Vilotte JP, Bevis M, Brooks B, Smalley R, Parra H, Baez JC, Blanco M, Cimbaro S and Kendrick E (2011), The 2010 Mw 8.8 Maule Megathrust Earthquake of Central Chile, Monitored by GPS, *Science*, 332(6036): 1417–1421. doi: 10.1126/science.1204132.